Exploration of Vanado-Phosphate Frameworks towards Electrochemical Water Oxidation Applications

Dissertation submitted to
Visvesvaraya National Institute of Technology, Nagpur
in partial fulfillment of the requirements for the award of
the degree

Master of Science

in

Chemistry

by

Sneha Mishra (MS23CHM018)

under the guidance of

Dr. Abhishek Banerjee

Department of Chemistry
Visvesvaraya National Institute of Technology
Nagpur 440010 (India)

2025

Exploration of Vanado-Phosphate Frameworks towards Electrochemical Water Oxidation Applications

Dissertation submitted to
Visvesvaraya National Institute of Technology, Nagpur
in partial fulfillment of the requirements for the award of
the degree

Master of Science

in

Chemistry

by

Sneha Mishra (MS23CHM018)

under the guidance of

Dr. Abhishek Banerjee

Department of Chemistry
Visvesvaraya National Institute of Technology
Nagpur 440010 (India)

2025

© Visvesvaraya National Institute of Technology (VNIT) 2009

Department of Chemistry

Visvesvaraya National Institute of Technology, Nagpur

Declaration

I, Sneha Mishra, hereby declare that this dissertation titled "**Exploration of Vanado-Phosphate Frameworks towards Electrochemical Water Oxidation Applications**" is carried out by me in the Department of Chemistry of Visvesvaraya National Institute of Technology, Nagpur. The work is original and has not been submitted earlier, whole or in part, for the award of any degree/diploma at this or any other Institution / University.

Date:

Certificate

This to certify that the dissertation titled "**Exploration of Vanado-Phosphate Frameworks towards Electrochemical Water Oxidation Applications**" is submitted by **Sneha Mishra** in partial fulfillment of the requirements for the award of the degree of **Master of Science in Chemistry**, VNIT Nagpur. The work is comprehensive, complete and fit for final evaluation.

Dr. Abhishek Banerjee
Assistant Professor
Department of Chemistry
VNIT, Nagpur

Head of the Department,
Department of Chemistry,
VNIT, Nagpur.
Date:

Non-Plagiarism Certificate

It is certified that the M.Sc. dissertation titled "**Exploration of Vanado-Phosphate Frameworks towards Electrochemical Water Oxidation Applications**" by **Sneha Mishra** bearing Enrollment No. MS23CHM018, ID-30683 has been examined by us with the following anti-plagiarism tools.

The thesis has been checked using TURNITIN (copy of originality report attached) and found within limits as per HEC plagiarism Policy and instructions issued from time to time.

Sneha Mishra

MS23CHM018

Dr. Abhishek Banerjee

Assistant Professor

Department of Chemistry

VNIT, Nagpur 440010

Acknowledgement

I would like to express my heartfelt gratitude to everyone who contributed to the success of this project. Firstly, I am deeply thankful to my supervisor, Dr. Abhishek Banerjee, whose unparalleled expertise, guidance, and support were invaluable throughout this period. His genuine interest and invaluable advice were crucial to my progress. I am also profoundly grateful to the Head of the Department, Dr. Sujit K Ghosh, for his dedication to science and research and for providing all necessary facilities until the end of this research. I acknowledge the Oxo-Thiometalate Lab, Dept of Chemistry, VNIT Nagpur, for their support in completing this project. Special thanks to the PhD scholars, Shikha Singh, Kalyan Morla and Sandeep Chaudhary, for their technical assistance and for nurturing me with their mental and moral support. I am forever indebted to them. I appreciate my colleagues and fellow mates for their collaboration, stimulating discussions, and camaraderie. Their constructive criticisms and shared knowledge guided me through this journey. Lastly, I want to express my heartfelt gratitude to my family for their unwavering support, belief, and blessings throughout my life. I am also grateful to the Almighty for giving me the strength to persevere through this time

Abstract

With the rising demand towards sustainable and cleaner energy sources, generation of hydrogen from water is one of the most important research activities. Hydrogen, with its exceptionally high gravimetric calorific value, is an excellent fuel towards energy generation. However, being gaseous, use of hydrogen has several challenges, which includes proper and safe storage, and use. One of the ways to mitigate such problems is to be able to generate hydrogen in situ from a high hydrogen density source. Out of the many sources of hydrogen, water is an excellent candidate, containing ideally two mols of hydrogen per mol of water. However, production of hydrogen from water requires a catalyst to overcome the potential of 1.23 V required for such a reaction. Thus, an efficient catalyst for water splitting must exhibit low overpotential, good electrical conductivity, and long-term stability in both acidic and alkaline environments, to effectively drive the hydrogen and oxygen evolution reactions. Oxo-vanadates, due to their considerable stability in multiple oxidation state(s) as well as coordination environment(s), are excellent candidates as effective electrocatalysts.

In this research project we explored two vanado-phosphate framework materials, the homo-valent $(C_4H_{10}N_2H_2)_{0.5}(C_4H_{10}N_2H)[V^{III}_4(HPO_3)_7(H_2O)_3]\bullet 1.5H_2O$ (**1**) and the mixed-valent$(H_3NCH_2CH_2NH_3)_4[V^{III}(H_2O)_2(V^{IV}O)_6(OH)_2(HPO_4)_3(PO_4)_5]\bullet 3H_2O$ (**2**), for electrochemical water splitting. The framework-type assembly provides additional stability towards such electrochemical processes. Both frameworks possess extensive channels, providing sufficient space for good ionic mobility. The synthesized compounds were extensively characterized using powder X-ray diffraction and infrared spectroscopic methods. Electrochemical performance studies were done in a three-electrode setup, and with cyclic voltammetry and linear sweep voltammetry, to understand the trend in HER performance. Lower overpotential and CV peak separation was observed in compound **1**, which exemplified easier electron transfer and more favorable reversible electrochemistry, in comparison with compound **2**. However, **2** gave larger negative current at 0.5 V, implying that it can push more current once active. These results show that overall compound **2** has better final catalytic current and catalytic turnover. Since lower overpotential is key criteria for better electrocatalyst, compound **1** is a better electrocatalyst to start significant current generation. However, compound **2** is better in sustaining the electrochemical process and overall yield.

List of Figures

Figure Caption	Page No.
Figure 1.1: Electrochemical profile for water oxidation catalysis	**3**
Figure 1.2: Current density *vs* Potential profile for electrocatalytic water oxidation	**5**
Figure 1.3: Type of oxo-vandates based upon coordination.	**6**
Figure 2.1: Ball-and-stick representation of Vanadium(III) phosphite $(C_4H_{10}N_2H_2)_{0.5}(C_4H_{10}N_2H)[V_4(HPO_3)_7(H_2O)_3]\bullet 1.5H_2O$ **(1)**	**9**
Figure 2.2: Ball-and-stick representation of Vanadium(III-IV) phosphate **(**$(H_3NCH_2CH_2NH_3)_4[V^{III}(H_2O)_2(V^{IV}O)_6(OH)_2(HPO_4)_3(PO_4)_5]\bullet 3H_2O$ **(2)**	**10**
Figure 2.3: Comparative IR spectra of $(C_4H_{10}N_2H_2)_{0.5}(C_4H_{10}N_2H)[V^{III}{}_4(HPO_3)_7(H_2O)_3]\bullet 1.5H_2O$ (**1**) and $(H_3NCH_2CH_2NH_3)_4[V^{III}(H_2O)_2(V^{IV}O)_6(OH)_2(HPO_4)_3(PO_4)_5]\bullet 3H_2O$ (**2**)	**11**
Figure 2.4: Comparative PXRD pattern of **(a)** $(C_4H_{10}N_2H_2)_{0.5}(C_4H_{10}N_2H)[V^{III}{}_4(HPO_3)_7(H_2O)_3]\bullet 1.5H_2O$ (**1**), and **(b)** $(H_3NCH_2CH_2NH_3)_4[V^{III}(H_2O)_2(V^{IV}O)_6(OH)_2(HPO_4)_3(PO_4)_5]\bullet 3H_2O$ (**2**)	**12**
Figure 3.1: Representation of the three-electrode setup	**14**
Figure 3.2: Schematic representation of electrode preparation	**15**
Figure 3.3: Prepared working electrode – electrocatalyst coated glassy carbon electrode	**15**
Figure 3.4: Cyclic voltammetry of homo-valent Vanado-Phosphite $(C_4H_{10}N_2H_2)_{0.5}(C_4H_{10}N_2H)[V^{III}{}_4(HPO_3)_7(H_2O)_3]\bullet 1.5H_2O$ (**1**)	**16**
Figure 3.5: Cyclic voltammetry of mixed-valent Vanadium Phosphate $(H_3NCH_2CH_2NH_3)_4[V^{III}(H_2O)_2(V^{IV}O)_6(OH)_2(HPO_4)_3(PO_4)_5]\bullet 3H_2O$ (**2**)	**17**

Figure 3.6: Linear sweep voltammetry of homo-valent Vanado-Phosphite $(C_4H_{10}N_2H_2)_{0.5}(C_4H_{10}N_2H)[V^{III}_4(HPO_3)_7(H_2O)_3]\bullet 1.5H_2O$ (**1**) **18**

Figure 3.7: Linear sweep voltammetry of mixed-valent Vanadium Phosphate $(H_3NCH_2CH_2NH_3)_4[V^{III}(H_2O)_2(V^{IV}O)_6(OH)_2(HPO_4)_3(PO_4)_5]\bullet 3H_2O$ (**2**) **19**

Figure 3.8: PXRD pattern of electrode material $(C_4H_8N_2H_4)_{0.5}(C_4H_8N_2H_3)[V_4(HPO_3)_7(H_2O)_3]\bullet 1.5H_2O$ (**1**) **(a)** Before, and **(b)** After electrochemistry **20**

Figure 3.9: PXRD pattern of electrode material $(H_3NCH_2CH_2NH_3)_4[V^{III}(H_2O)_2(V^{IV}O)_6(OH)_2(HPO_4)_3(PO_4)_5]\bullet 3H_2O$ **(2) (a)** Before, and **(b)** After electrochemistry **20**

Abbreviations

POM	Polyoxometalate
POV	Polyoxovanadate
HER	Hydrogen evolution reaction
OER	Oxygen evolution reaction
CV	Cyclic voltammogram
LSV	Linear sweep voltammogram

Contents

Abstract vi

List of Figures vii

Abbreviations ix

CHAPTER 1: INTRODUCTION 1

1.1 Brief Discussion on Kinetics, Thermodynamics and Mechanism of electrochemical water splitting 3

1.2 Role of Electrocatalyst 5

1.2.1 Why Vanadiun-based Electrocatalyst is a Good Choice for Electrocatalytic Water Oxidation 5

1.3 Oxo-Vanadates 6

1.4: Outlook of current research project 7

CHAPTER 2: SYNTHESIS, STRUCTURE AND CHARACTERISATION 9

2.1 Synthesis of homo-valent oxo-vanado(III)-phosphite 10

2.2 Synthesis of mixed-valent oxo-vanado(III)-phosphate 10

2.3 Structural details 11

2.3.1 $(C_4H_{10}N_2H_2)_{0.5}(C_4H_{10}N_2H)[V_4(HPO_3)_7(H_2O)_3]\bullet 1.5H_2O$ (1) 11

2.3.2 $(H_3NCH_2CH_2NH_3)_4[V^{III}(H_2O)2(V^{IV}O)_6(OH)_2(HPO_4)_3(PO_4)_5]\bullet 3H_2O$ (2) ... 11

2.4 Characterization of oxo-vanado-phosphates 12

2.4.1 Infrared Spectroscopy 12

2.4.2 Powder X-ray diffraction 13

CHAPTER 3: RESULTS AND DISCUSSION - ELECTROCHEMICAL STUDIES 14

3.1 Components of Electrochemical water splitting setup 15

3.2 Preparation of working electrode – electrocatalyst coated electrode 16

3.3 Electrochemical Activity Study of Electrocatalysts 17

3.3.1 Cyclic voltammetry (CV) 17

(a) $(C_4H_{10}N_2H_2)_{0.5}(C_4H_{10}N_2H)[V^{III}_4(HPO_3)_7(H_2O)_3]\bullet 1.5H_2O$ (1) 17

(b) $(H_3NCH_2CH_2NH_3)_4[V^{III}(H_2O)_2(V^{IV}O)_6(OH)_2(HPO_4)_3(PO_4)_5]\bullet 3H_2O$ (2) .. 18

3.3.2 Linear Sweep Voltammetry 18

(a) $(C_4H_8N_2H_4)_{0.5}(C_4H_8N_2H_3)[V_4(HPO_3)_7(H_2O)_3]\bullet 1.5H_2O$ (1) 19

(b)$(H_3NCH_2CH_2NH_3)_4[V^{III}(H_2O)_2(V^{IV}O)_6(OH)_2(HPO_4)_3(PO_4)_5]\bullet 3H_2O$ (2) ... 19

3.3.3 Characterization of electrode material – Before and After Electrochemical Analysis 20

(a) $(C_4H_8N_2H_4)_{0.5}(C_4H_8N_2H_3)[V_4(HPO_3)_7(H_2O)_3]\bullet 1.5H_2O$ (1) 21

(b) $(H_3NCH_2CH_2NH_3)_4[V^{III}(H_2O)_2(V^{IV}O)_6(OH)_2(HP\ O_4)_3(PO_4)_5]\bullet 3H_2O$ (2) . 21

CHAPTER 4: CONCLUSION 22

CHAPTER 1: INTRODUCTION

1. INTRODUCTION

With increasing global energy demand for green energy sources, this has accelerated the search for clean, renewable, and sustainable energy sources. Among all, hydrogen (H_2) has emerged as a highly promising candidate towards energy generation, due to its exceptionally high gravimetric calorific value. This is also why hydrogen is considered as a turning point in the development of a carbon-neutral energy economy, as zero carbon emissions occurs upon its combustion.

Being gaseous, use of hydrogen has several challenges, which includes proper and safe storage and use. Out of the many sources of hydrogen, water is an excellent candidate, containing ideally two mols of hydrogen per mol of water. One of the most sought-after research problems is therefore the extraction of hydrogen from water in a cost effective and efficient process. Extraction of hydrogen from water thus involves the breaking of hydrogen-oxygen bonds, *i.e.* water splitting. There are basically 3 kinds of water splitting techniques known, (i) Photochemical [PC], (ii) Photoelectrochemical [PEC], and (iii) Photovoltaic electrolysis [PVE]. PEC is most attractive and substantial way.

In 1972, Fujishima and Honda first used TiO_2 photoanode for PEC water splitting in presence of UV light irradiation. In PEC cell solar water-splitting is done by use of semiconducting photoelectrodes and one metallic (dark) electrode. The use of non-noble metal catalysts in place of high price and rare noble metal catalysts have been developed. But high electricity consumption, low efficiency, and large overpotential through a sluggish anodic OER (oxygen evolution reaction) and a relatively facile cathodic HER (hydrogen evolution reaction) has led towards great impetus towards designing effective electrocatalysts with overall low over-potential, high activity, stability, higher conversion efficiency, low cost, simpler, easy synthesis, environment friendly, and space saving construction.

Electrochemical water splitting involves two half-reactions:

- **Hydrogen Evolution Reaction (HER)** at the cathode
- **Oxygen Evolution Reaction (OER)** at the anode.

requiring a minimum of 1.23V for water splitting. But in practice, higher voltages than this are necessary due to kinetic barriers. Thus, the use of electrocatalysts is essential to reduce the overpotential and improve the reaction efficiency [depicted in **Figure 1.1**].

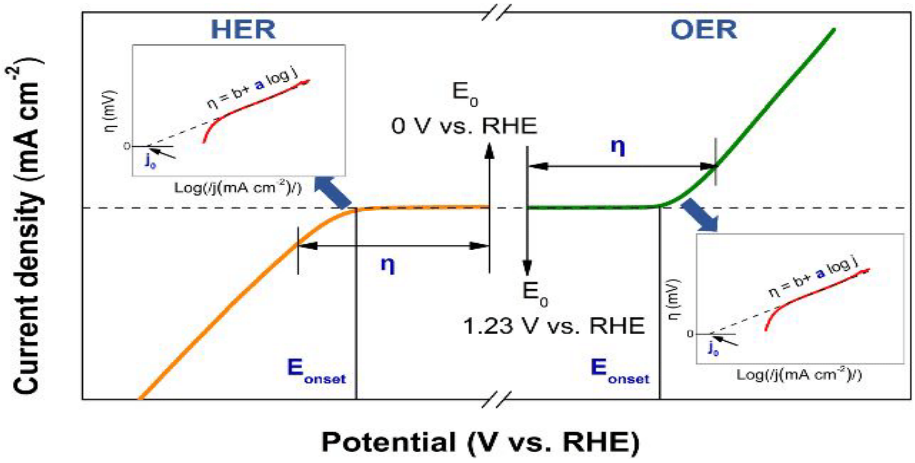

Figure 1.1: Electrochemical profile for water oxidation catalysis

Although noble metals such as Pt and IrO_2 are very effective, but their high cost and limited availability limits their large-scale application. This has prompted search for earth abundant alternatives with comparable performances, and so we move towards Transition metal-based alternatives, due to their:

- Abundance
- Multiple oxidation states, and
- Electronic versatility.

It has been also observed that transition metal-based chalcogenides, carbides, nitrides, and phosphides show significance as HER electrocatalysts, whereas transition metal-based hydroxides, oxyhydroxides, or incorporation with other metalloids (N, S, P, B, Se etc.) show better efficiency for OER.

1.1 Brief Discussion on Kinetics, Thermodynamics and Mechanism of electrochemical water splitting

This process involves breaking of O-H bond and generation of hydrogen gas when sufficient external potential is applied. It consists of two half-reactions:

- **Hydrogen Evolution Reaction (HER)** at the cathode
- **Oxygen Evolution Reaction (OER)** at the anode.

The reaction requires **Standard Gibbs free energy** (ΔG_o) of 237.2 kJ/mol at 25 ^{0}C and 1 atm pressure and theoretical **Standard cell potential** (E^0) of 1.23 V (vs RHE). However, due to energy losses (kinetic barrier), a higher actual voltage, approximately in the range of 1.6-2.0 V is required.

Hydrogen evolution reaction (HER) process is a cathodic reaction in water electrolysis, contains 2-electron transfer process with the production of one molecule of H_2. General reaction mechanism of HER in acidic and alkaline solution is given below:

Electrochemical hydrogen adsorption (Volmer reaction)

$$H^+ + M + e^- \rightleftharpoons M-H* \quad (acidsolution)$$

$$H_2O + M + e^- \rightleftharpoons M-H* + OH^- (alkalinesolution)$$

H* indicate chemically adsorbed hydrogen and M indicate electrode surface.

Electrochemical desorption (Heyrovsky reaction)

$$M-H* + H^+ + e^- \rightleftharpoons M + H_2 (acidsolution)$$

$$M-H* + H_2O + e^- \rightleftharpoons M + OH^- + H_2\ (alkalinesolution)$$

or, chemical desorption (Tafel reaction)

$$2M-H* \rightleftharpoons 2M + H_2 (bothacidandalkalinesolution)$$

The above reactions are possible rate controlling steps and distinguished by Tafel slope.

Oxygen evolution reaction (OER) at anode is a 4-electron process generating one mole of oxygen. Here, noble metal-based catalysts (like Ir, Ru) prefer acidic media, where transition metal (Fe, Co, and Ni) prefer alkaline electrolyte. The presence of elementary steps with adsorption intermediates (OOH*, O*, and OH*) make the process sluggish than HER. The mechanism is as follows:

Step 1: $OH^- + * \rightarrow HO^* + e^-$

Step 2: $HO^* + OH^- \rightarrow O^* + H_2O + e^-$

Step 3: $O^* + OH^- \rightarrow HOO^* + e^-$

Step 4: $HOO^* + OH^- \rightarrow * + O_2 + H_2O + e^-$

1.2 Role of Electrocatalyst

An effective electrocatalyst should exhibit the following properties:

- Low overpotential
- High electrical conductivity
- Chemical and structural stability in both, acidic and alkaline environments
- Good catalytic turnover
- High durability
- Offer accessible active sites and porous structure for reactant transport

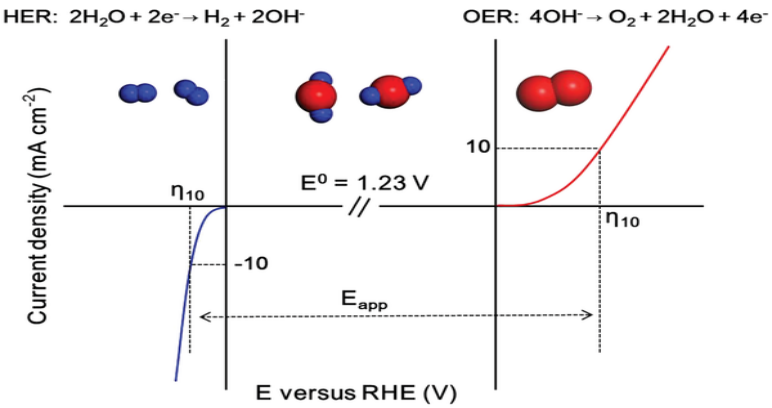

Figure 1.2: Current density *vs* Potential profile for electrocatalytic water oxidation

1.2.1 Why Vanadiun-based Electrocatalyst is a Good Choice for Electrocatalytic Water Oxidation

Studies show that Vanadium based electrocatalysts exhibit promising properties due to:

- It's wide redox window (V^{+2} to V^{+5})
- Flexible coordination geometries
- Good electronic properties for redox based catalysts

However, their performance is generally limited by poor conductivity and low stability. However, combination of oxo-vanadates with elements such as Phosphorous, Nitrogen, Sulphur or Oxygen form hybrid structure of Phosphites, Sulphides and Oxides exhibiting improved catalytic properties. This is why researchers started exploring Vanado-

Phosphate Frameworks, which are crystalline compounds that have combined vanadium centers with phosphate groups, generally in a network orientation. Additional benefits of Vanado-Phosphate Frameworks are:

- **Framework stability** from strong V-O-P bonding
- **Tunable porosity and active site exposure**
- **Redox versatility** shown by mixed-valence V centers
- **Hydrophilic channels** for ion transport

1.3 Oxo-Vanadates

These are subclass of polyoxometalates that consists of vanadium as center atom coordinated with oxygen in various geometries, varying from tetrahedral $\{VO_4\}$, square-pyramidal $\{VO_5\}$, to octahedral $\{VO_6\}$ [**Figure 1.3**]. They are classified under 2 sub-groups: (1) iso-polyvanadates, e.g. $[V_{10}O_{28}]^{6-}$, and (2) hetero-polyvanadates, e.g. $[V_5O_6(OCH_3)_{12}Fe(ClO_4)]$. Coordination geometry of individual vanadium atom exhibits cage, sphere, hollow, basket, belt, and barrel-like structural motifs, constructed by a number of polyhedra fused and/or linked through a common vertex, edges and faces.

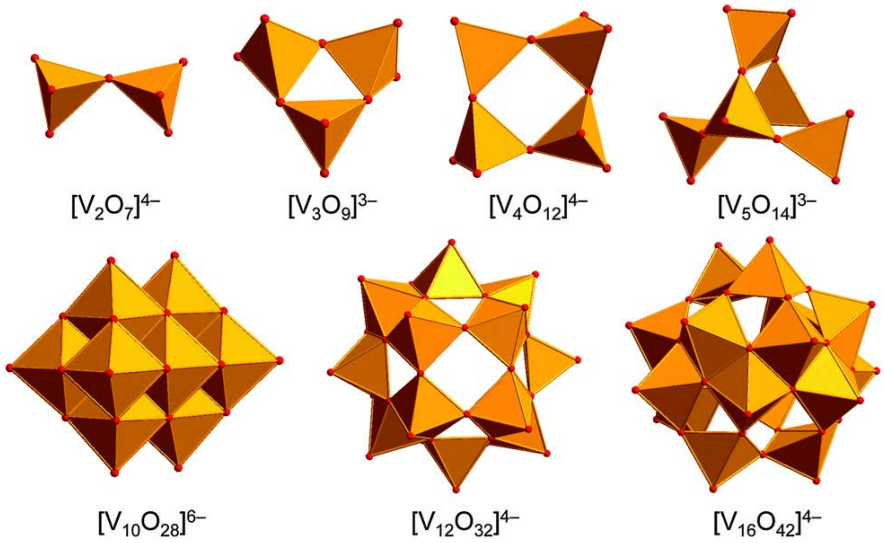

Figure 1.3: Type of oxo-vandates based upon coordination.

Vanadium shows variable oxidation states such as +2 (lilac/purple), +3 (green), +4 ($\{V^{IV}O\}^{2+}$, blue), +5 ($\{V^{V}O_2\}^{+}$ and $\{V^{V}O_3\}$, yellow). Based upon the oxidation-state, oxo-vanadatescan be thus be broadly classified into four families – fully oxidized oxo-vanadates (V^{V}), the reduced oxo-vanadates (V^{IV}), substantially reduced oxo-vanadate

(V^{III}), and mixed-valent oxo-vanadate (V^{V}/V^{IV} or V^{IV}/V^{III}). The most characteristic features of oxo-vanadates are high stability and wide redox profile, ranging from (V^{+3},V^{+4} and V^{+5}), which is responsible for high co-ordinational and redox flexibility. Additionally, the strong V–O bonds provide structural robustness under both acidic and alkaline conditions, enhancing the chemical and thermal stability of the catalyst.

Therefore, in context of electrochemical water splitting, oxo-vanadates serve as promising candidates for effective electrocatalyst as it is abundant, low cost, facilitates fast electron transfer, offer porosity and accessible channels (improving ion diffusion and active site exposure), show low overpotential, have high catalytic current density and good durability.

1.4: Outlook of current research project

Aiming to explore oxo-vanadate frameworks for electrochemical water oxidation catalysis, the following research strategy was adopted.

- Synthesis of inorganic phospho-vanadate anionic frameworks, stabilized by organic counter-cations.
- Characterization of synthesized compounds using powder X-ray diffraction, infrared spectroscopy.
- Immobilization of synthesized compounds onto electrode surface. Studies into electrochemical water splitting with prepared electrodes

1.5: References:

[1] “B. J. Ng, L. K. Putri, X. Y. Kong, Y. W. Teh, P. Pasbakhsh, S. P. Chai. Z-Scheme”.

[2] “K. F. Chin, M. Đokić, H. S. Soo. Artificial Photosynthesis beyond Water Splitting for”.

[3] “S. T. Kochuveedu. Photocatalytic and Photoelectrochemical water splitting on TiO2 via”.

[4] “ Y. Zhang, J. Liu, S. -L. Li, Z. -M. Su, Y. -Q. Lan. Polyoxometalate-based materials for”.

[5] “Y. Zhao, J. R. Swierk, J. D. Megiatto Jr. et al. Improving the efficiency of water splitting in”.

[6] “A. Kudo, Y. Miseki. Heterogeneous photocatalyst materials for water splitting. Chemical”.

[7] “Y. Zhang, J. Liu, S. -L. Li, Z. -M. Su, Y. -Q. Lan. Polyoxometalate-based materials for”.

[8] “A. Hiskia, A. Mylonas, E. Papaconstantinou. Comparison of the photoredox properties of”.

[9] “C. L. Hill, D.A. Bouchard. Catalytic photochemical dehydrogenation of organic substrates by”.

[10] “. D. A. Friesen, J. V. Headley and C. H. Langford. New On-line Mass Spectrometer for”.

[11] “R.-K. Chiang, N.-T. Chuang; Journal of Solid State Chemistry, 2005, 178, 3040–3045”.

[12] “A.J. Cortese et al.; Solid State Sciences, 2016, 60, 59-64”.

[13] “R.-K. Chiang, N.-T. Chuang; Journal of Solid State Chemistry, 2005, 178, 3040–3045”.

[14] “A.J. Cortese et al.; Solid State Sciences, 2016, 60, 59-64”.

[15] “R.-K. Chiang, N.-T. Chuang; Journal of Solid State Chemistry, 2005, 178, 3040–3045”.

[16] “Harrison, W.T.A.; Chem. Mater. 1995, 7, 2004-2006”.

[17] “ M. Schindler, F.C. Hawthorne, W.H. Baur, Chem. Mater. 12”.

[18] “A.M. Chippindale, Chem. Mater. 12 (2000) 818”.

[19] “W.T.A. Harrison, K. Hsu, A.J. Jacobson, Chem. Mater. 7 (1995)”.

[20] “Y.M. Tsai, S.L. Wang, C.H. Huang, K.H. Lii, Inorg. Chem. 38”.

[21] “W.T.A. Harrison, K. Hsu, A.J. Jacobson, Chem. Mater. 7 (1995)”.

[22] X. Li, X. Hao, A. Abudula, G. Guan. Nanostructured catalysts for electrochemical water splitting: current state and prospects. Journal of Materials Chemistry A, 2016, 4, 11973-12000.

[23] “A.M. Chippindale, S.J. Brech, A.R. Coeley, W.M. Simpson,”.

CHAPTER 2: SYNTHESIS, STRUCTURE AND CHARACTERISATION

2. SYNTHESIS, STRUCTURE AND CHARACTERIZATION

For our electrocatalytic studies, two vanado-phosphate structures, homo-valent and mixed-valent, were selected from the literature and their synthesis were performed as per reported literature procedure.

2.1 Synthesis of homo-valent oxo-vanado(III)-phosphite

To 0.070 g of V_2O_5 taken in 8mL H_2O, to which 1.0 g of H_3PO_3 was added with constant stirring, followed by the addition of 0.78 g of piperazine. Molar composition of initial mixture was V_2O_5 : H_3PO_3 : piperazine : H_2O is 1:30:10:1110. This mixture was stirred for 30 min and then heated at 170 ^{0}C for 4 days in a Teflon-lined stainless-steel autoclave under autogenous pressure, further cooled slowly to ambient temperature. Light-green crystals of compound **$(C_4H_8N_2H_4)_{0.5}(C_4H_8N_2H_3)[V_4(HPO_3)_7(H_2O)_3]\bullet1.5H_2O$** were collected by filtration, washed with distilled water, and air-dried. The yield of product was 40% in weight based on vanadium.

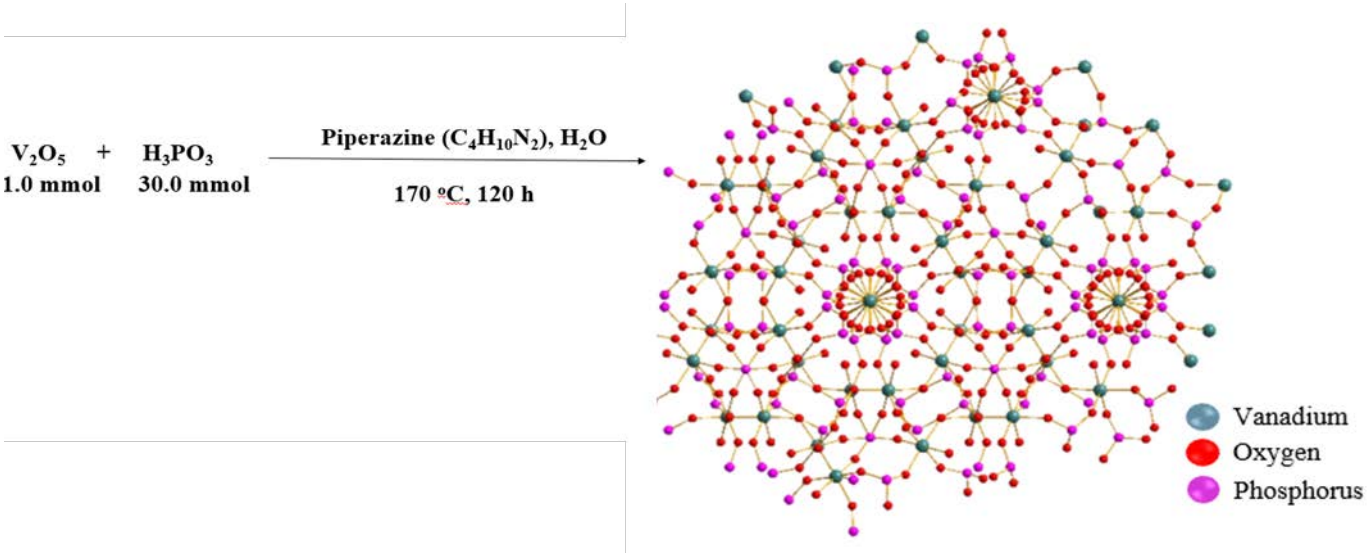

Figure 2.1: Ball-and-stick representation of Vanadium(III) phosphite **$(C_4H_{10}N_2H_2)_{0.5}(C_4H_{10}N_2H)[V_4(HPO_3)_7(H_2O)_3]\bullet1.5H_2O$ (1)**

2.2 Synthesis of mixed-valent oxo-vanado(III)-phosphate

Molar composition ratio of mixture V_2O_5 : H_3PO_4 : $H_2NCH_2CH_2NH_2$: H_2O in the mol ratio of 1 : 6.9 : 3.6 : 265 was kept in a Teflon-lined stainless-steel autoclave and heated at 170^{0}C for 5 days hydrothermally. Blue bipyramidal-shaped crystals of compound

$(H_3NCH_2CH_2NH_3)_4[V^{III}(H_2O)2(V^{IV}O)_6(OH)_2(HPO_4)_3(PO_4)_5]\bullet 3H_2O$ were obtained with a 57% yield.

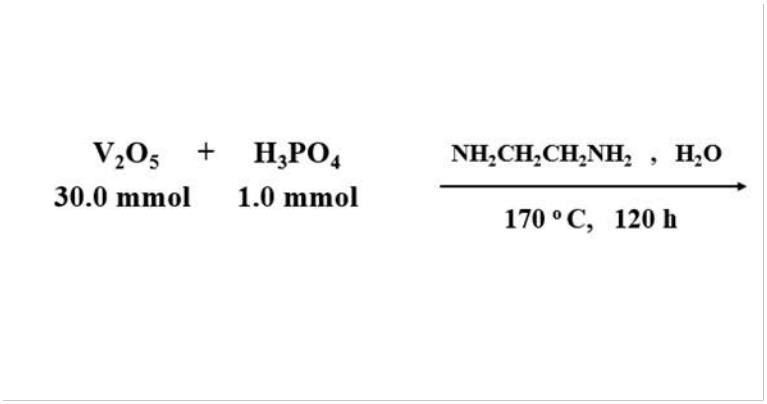

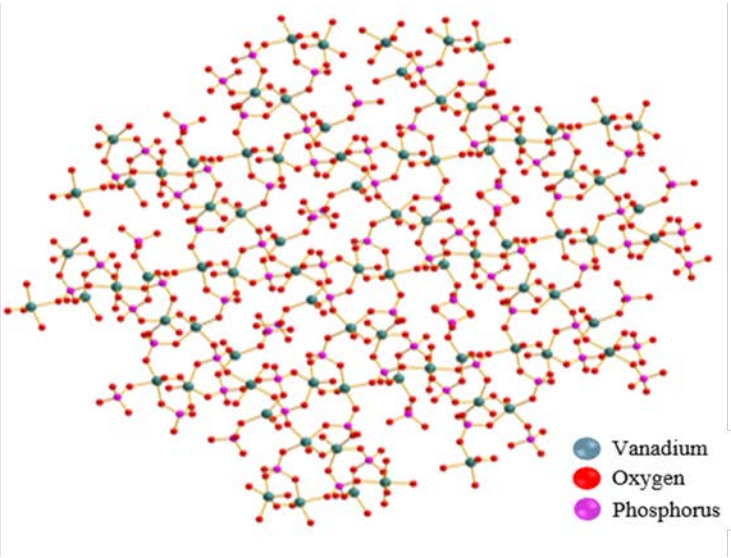

Figure 2.2: Ball-and-stick representation of Vanadium(III-IV) phosphate **$(H_3NCH_2CH_2NH_3)_4[V^{III}(H_2O)_2(V^{IV}O)_6(OH)_2(HPO_4)_3(PO_4)_5]\bullet 3H_2O$ (2)**

2.3 Structural details

2.3.1 $(C_4H_{10}N_2H_2)_{0.5}(C_4H_{10}N_2H)[V_4(HPO_3)_7(H_2O)_3]\bullet 1.5H_2O$ (1)

The structure of the compound consists of 3D open-framework with intersecting 12-member ring channels, with protonated piperazine cations and water molecules present in the channels. The 2D sheets with 4,6-member rings of vanadium-centric VO_6, $VO_5(H_2O)$ and phosphorous-centric HPO_3 units are formed first, which are then linked together by sharing vertex-oxygen atoms of $\{VO_6\}$ units generating a 3D open-framework structure. Here, piperazine plays role of an organic template in the synthesis. All of vanadium atoms are in octahedral environment formed by six O atoms with an average V–O bond length of 2.008A˚, which is typical for vanadium(III).

2.3.2 $(H_3NCH_2CH_2NH_3)_4[V^{III}(H_2O)2(V^{IV}O)_6(OH)_2(HPO_4)_3(PO_4)_5]\bullet 3H_2O$ (2)

This compound is an ethylenediamine encapsulated open-framework vanadium phosphate. In the mixed-valent compound, V(III) is in octahedral and V(IV) is in square pyramidal environment bridged by μ_2-OH groups, with phosphate (HPO_4^{2-}) and phosphate (PO_4^{3-}) ligands. Tunnels are occupied by ethylenediammonium and water

molecules. Ethylenediammonium ions acts as structure-directing agents and stabilizes the open framework structure. Tetrahedral PO_4 units bridge multiple V centers.

2.4 Characterization of oxo-vanado-phosphates

2.4.1 Infrared Spectroscopy

The IR spectra of both the compounds showed characteristic peaks from vanadate, phosphate and organic counter cations. Large band at 3430 cm^{-1} arises from O–H and N–H stretching vibrations, the intense bands at 1115 and 996 cm^{-1} were associated with the stretching vibrations of V–O and P–O bonds, respectively. Absorptions at 2388 cm^{-1} as well due to the stretching vibrations of the P–H groups in phosphate.

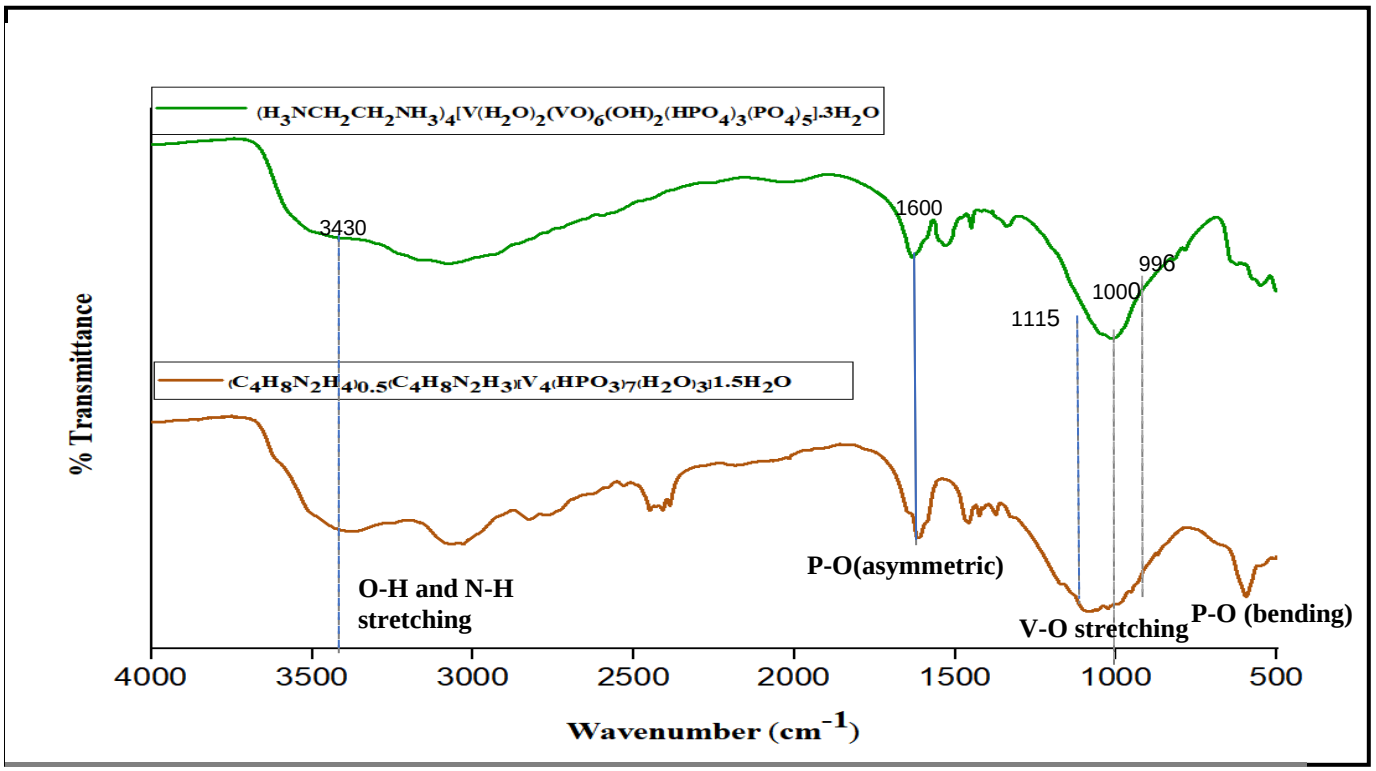

Figure 2.3: Comparative IR spectra of $(C_4H_{10}N_2H_2)_{0.5}(C_4H_{10}N_2H)[V^{III}_4(HPO_3)_7(H_2O)_3]\bullet 1.5H_2O$ (**1**) and $(H_3NCH_2CH_2NH_3)_4[V^{III}(H_2O)_2(V^{IV}O)_6(OH)_2(HPO_4)_3(PO_4)_5]\bullet 3H_2O$ (**2**)

2.4.2 Powder X-ray diffraction

Phase purity of both compounds was concluded by comparing the experimental *vs* simulated data.

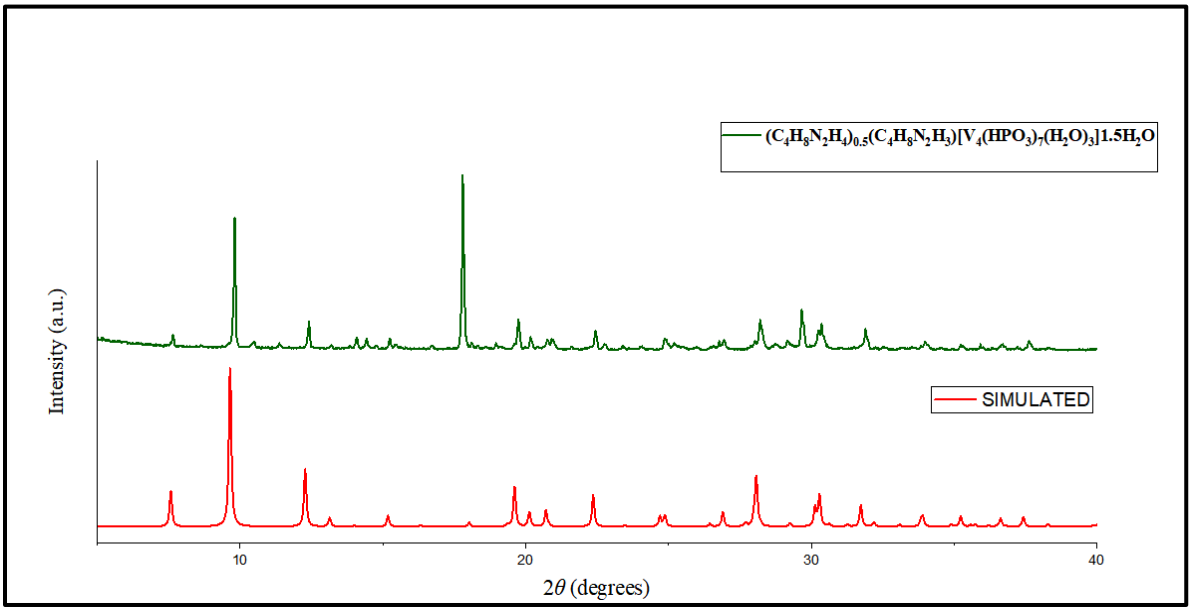

(a)

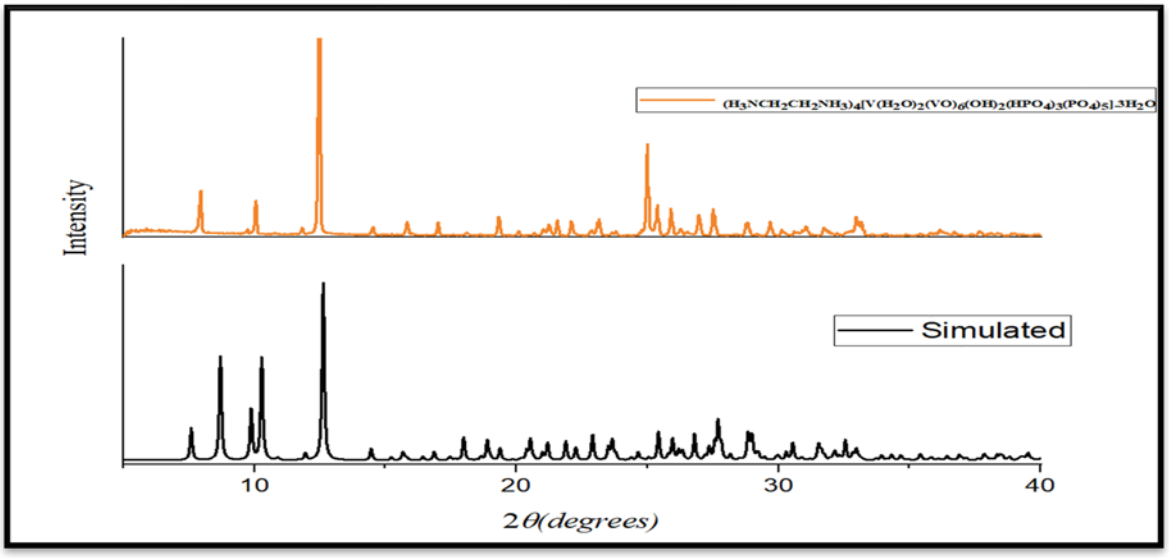

(b)

Figure 2.4: Comparative PXRD pattern of **(a)**$(C_4H_{10}N_2H_2)_{0.5}(C_4H_{10}N_2H)[V^{III}_4(HPO_3)_7(H_2O)_3]\bullet 1.5H_2O$ (**1**), and **(b)** $(H_3NCH_2CH_2NH_3)_4[V^{III}(H_2O)_2(V^{IV}O)_6(OH)_2(HPO_4)_3(PO_4)_5]\bullet 3H_2O$ (**2**)

CHAPTER 3: RESULTS AND DISCUSSION - ELECTROCHEMICAL STUDIES

3. RESULTS AND DISCUSSION

In this section we discuss the electrochemical water oxidation catalysis, through a series of controlled experiments aimed at evaluating the catalytic activity and stability of the synthesized materials. Cyclic voltammetry (CV) with varying scan rates was performed to analyze the electrochemical behavior of the oxo-vanadate materials. Linear sweep voltammetry (LSV) was employed to determine the onset potential and overpotential at a benchmark current density of 10 mA cm^{-2}, providing a measure of catalytic efficiency. Tafel slope analysis was used to gain insight into the reaction kinetics,

3.1 Components of Electrochemical water splitting setup

A three-electrode setup was employed for all the electrochemical experiments

- Working Electrode (WE): Glassy Electrode carbon
- Counter Electrode (CE): Pt electrode
- Reference Electrode (RE): Ag/AgCl (3M KCl)

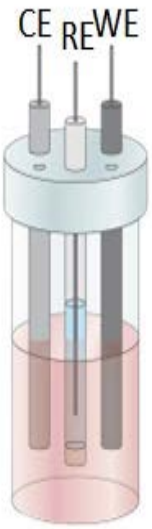

Figure 3.1: Representation of the three-electrode setup

ELECTROLYTE: Electrolytes that were used for electrochemical water splitting are Sulphuric acid **(**H_2SO_4), Potassium hydroxide (KOH) and Potassium phosphate buffer(KH_2PO_4 and K_2HPO_4). The objective of using the buffer is to maintain the pH of the system throughout the electrochemical study.

CATALYST: Facilitates hydrogen evolution reaction (HER) at cathode and oxygen evolution reaction (OER) at anode so it needs to have good redox profile.

3.2 Preparation of working electrode – electrocatalyst coated electrode

For preparation of desired electrode, a glassy carbon electrode (GCE) was modified using the drop casting method. Initially, respective compounds in very fine state and binder (Nafion) were mixed in a ratio of **4:1**, this ratio was found out by optimization. This mixture was dissolved in Ethanol and drop casted onto pre-cleaned surface of GCE. The drop was allowed to spread and adhere to its surface. The electrode was then dried under ambient conditions or using mild heat of IR lamp, ensuring uniform film formation and solvent evaporation.

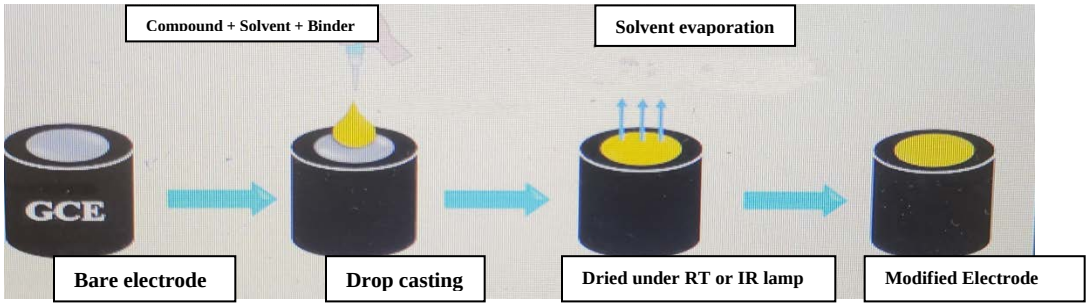

Figure 3.2: Schematic representation of electrode preparation

Figure 3.3: Prepared working electrode – electrocatalyst coated glassy carbon electrode

3.3 Electrochemical Activity Study of Electrocatalysts

3.3.1 Cyclic voltammetry (CV)

Cyclic voltammetry is an electrochemical technique that is used to study the redox behavior of a compound. Here, the potential was ramped from an initial value to set vertex potential and then revered back to the initial value, forming a triangular waveform. The resulting current response (represented on Y axis) is plotted against the applied potential (represented on X axis), producing a cyclic voltammogram.CV gave us an idea about the redox behavior, kinetics of electron transfer, electrochemical surface area, reaction reversibility, catalytic activity and stability of the compound.

(a) $(C_4H_{10}N_2H_2)_{0.5}(C_4H_{10}N_2H)[V^{III}_4(HPO_3)_7(H_2O)_3]\bullet 1.5H_2O$ (1)

We observe that the current ranges from -0.2 to +0.0012 A. This means the onset potential value is -0.2 A. Wide hysteresis between forward and backward scans indicate that electrocatalyst tends to show high capacitive behavior. Rectangular shape in center region indicates that the electrocatalyst has a large electrochemical surface area (ECSA), which means it has more active catalytic sites available for reaction to proceed. Peak separation is smaller than that of mixed-valent compound, indicating better reversibility.

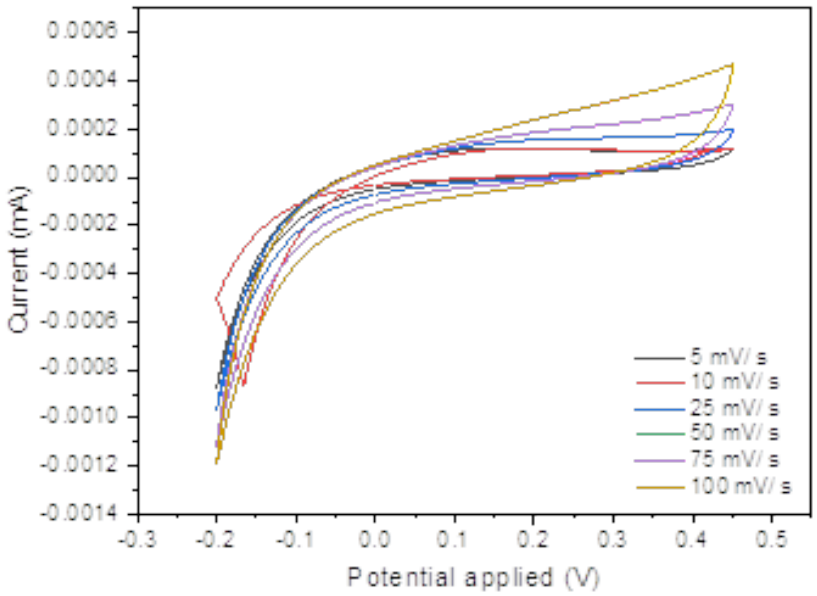

Figure 3.4: Cyclic voltammetry of homo-valent Vanado-Phosphite $(C_4H_{10}N_2H_2)_{0.5}(C_4H_{10}N_2H)[V^{III}_4(HPO_3)_7(H_2O)_3]\bullet 1.5H_2O$ (**1**)

(b) $(H_3NCH_2CH_2NH_3)_4[V^{III}(H_2O)_2(V^{IV}O)_6(OH)_2(HPO_4)_3(PO_4)_5]\cdot 3H_2O$ (2)

We observe that the current ranges from -0.0007 A to +0.0004 A. Comparatively narrower and tighter curves indicate towards less hysteresis and lower capacitive behavior. Smaller electrochemical surface area (ECSA) than former homo-valent compound, as there is an absence of rectangular region in the curve. Peak separation is comparatively larger, indicating lesser reversibility.

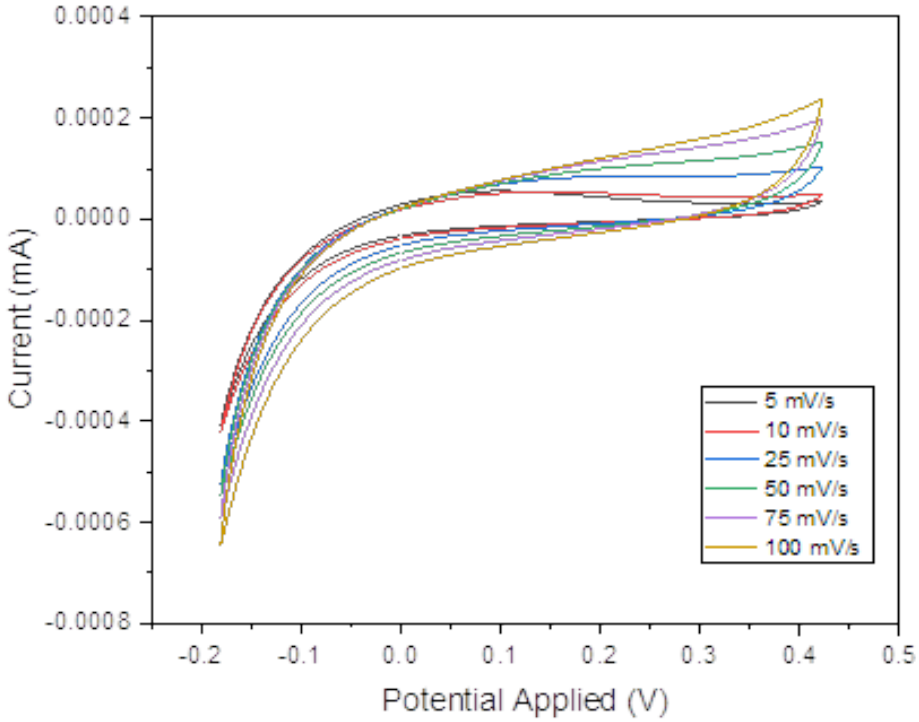

Figure 3.5: Cyclic voltammetry of mixed-valent Vanadium Phosphate $(H_3NCH_2CH_2NH_3)_4[V^{III}(H_2O)_2(V^{IV}O)_6(OH)_2(HPO_4)_3(PO_4)_5]\cdot 3H_2O$ (**2**)

3.3.2 Linear Sweep Voltammetry

Linear Sweep Voltammetry (LSV) is an electrochemical technique used to evaluate the behavior of electrocatalysts, particularly in reactions like oxygen evolution reaction (OER), hydrogen evolution reaction (HER), and oxygen reduction reaction (ORR). It involves sweeping of potential (V vs reference electrode) which is applied to the working electrode (represented on X axis) vary linearly with time, while measuring the resulting current (represented on Y axis). Thus, varying of potential is in one direction. LSV gives us an idea about the Onset potential, overpotential, Tafel analysis, current density and catalytic stability with repeated scans.

(a) $(C_4H_8N_2H_4)_{0.5}(C_4H_8N_2H_3)[V_4(HPO_3)_7(H_2O)_3]\bullet 1.5H_2O$ (1)

We observe that the current density drops sharply after approximately 0.2 – 0.3 V. Current reaches to about -0.12 mA at around 0.5 V, i.e. it shows negative current, which is a preferable indication for reduction processes like HER. The overpotential window for homo-valent compound starts around (0.2 – 0.25) V. This means at and beyond 0.2 V the electrocatalyst starts catalysis process

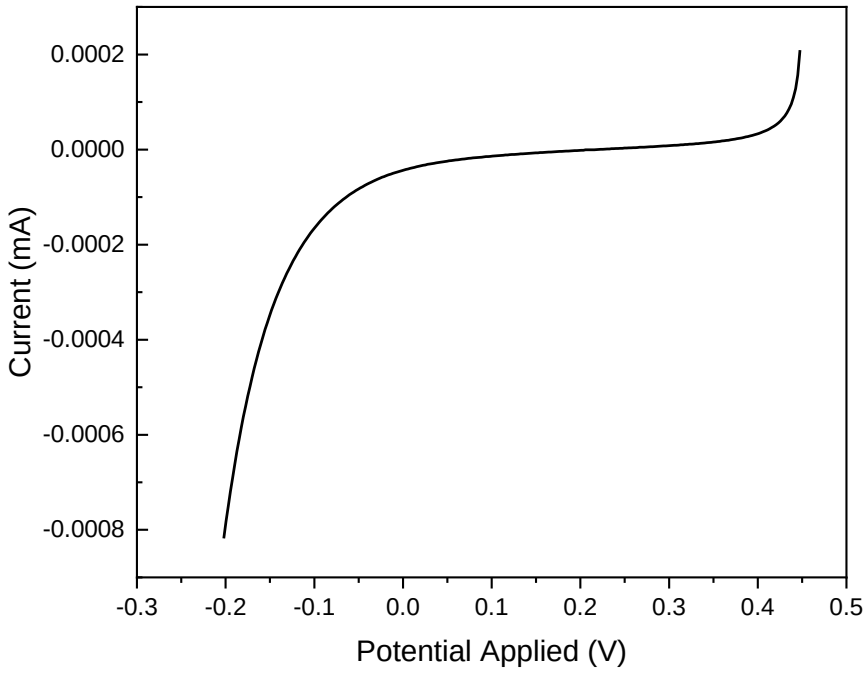

Figure 3.6: Linear sweep voltammetry of homo-valent Vanado-Phosphite $(C_4H_{10}N_2H_2)_{0.5}(C_4H_{10}N_2H)[V^{III}_4(HPO_3)_7(H_2O)_3]\bullet 1.5H_2O$ (**1**)

(b)$(H_3NCH_2CH_2NH_3)_4[V^{III}(H_2O)_2(V^{IV}O)_6(OH)_2(HPO_4)_3(PO_4)_5]\bullet 3H_2O$ (2)

We observe that current density drops sharply after approximately 0.30 V. The overpotential window for this mixed-valent compound starts around (0.30 – 0.33) V. This means at and beyond 0.30 V the electrocatalyst starts catalysis process. This is comparatively higher than homo-valent compound

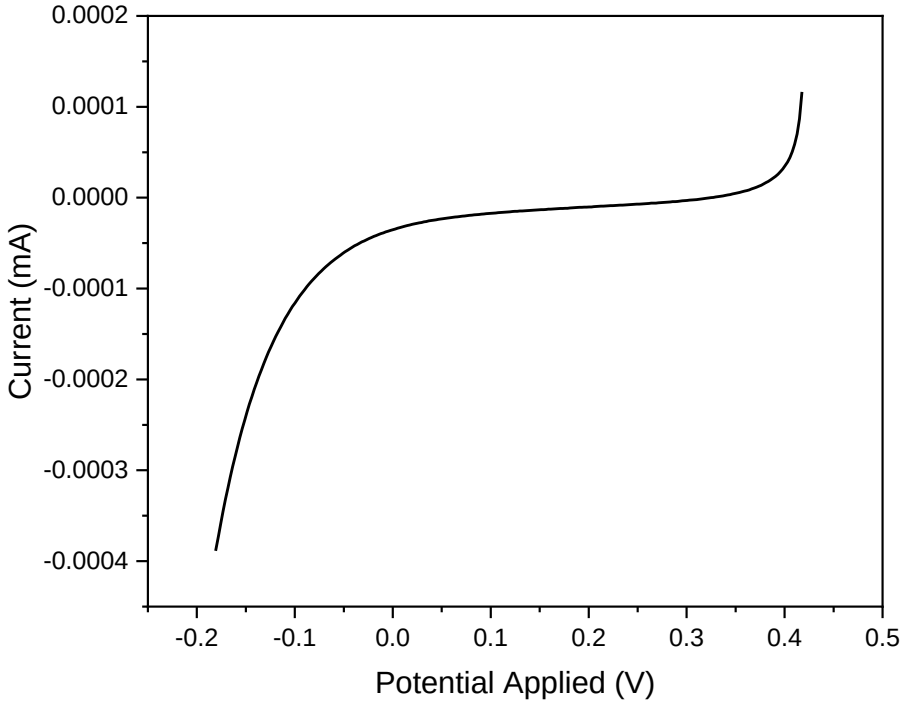

Figure 3.7: Linear sweep voltammetry of mixed-valent Vanadium Phosphate $(H_3NCH_2CH_2NH_3)_4[V^{III}(H_2O)_2(V^{IV}O)_6(OH)_2(HP\ O_4)_3(PO_4)_5]\bullet 3H_2O$ (**2**)

3.3.3 Characterization of electrode material – Before and After Electrochemical Analysis

Collecting PXRD of the electrode material before and after electrolysis is essential to assess any structural changes or phase transformations that may occur during catalytic operation, which can directly impact stability and performance.

From PXRD data collected both compounds, the homo-valent $(C_4H_{10}N_2H_2)_{0.5}(C_4H_{10}N_2H)[V^{III}{}_4(HPO_3)_7(H_2O)_3]\bullet 1.5H_2O$ (**1**) and the mixed-valent$(H_3NCH_2CH_2NH_3)_4[V^{III}(H_2O)_2(V^{IV}O)_6(OH)_2(HPO_4)_3(PO_4)_5]\bullet 3H_2O$ (**2**), were observed to retain their phase crystallinity and phase purity.

(a) $(C_4H_8N_2H_4)_{0.5}(C_4H_8N_2H_3)[V_4(HPO_3)_7(H_2O)_3]\bullet 1.5H_2O$ (1)

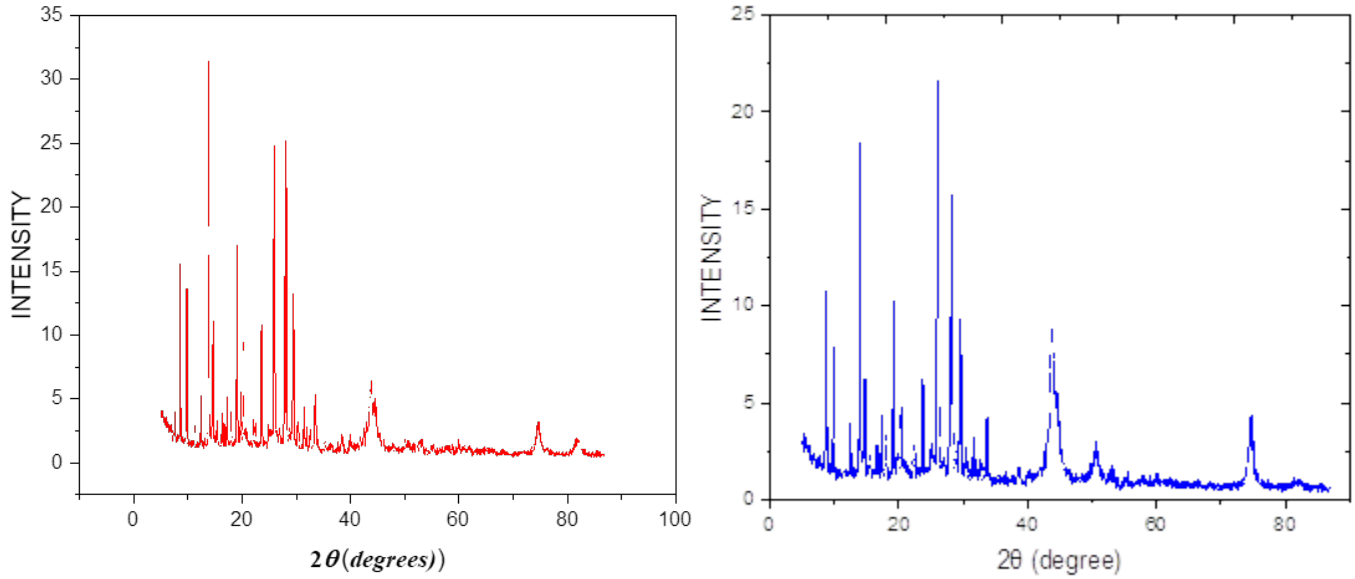

(a) **(b)**

Figure 3.8: PXRD pattern of electrode material $(C_4H_8N_2H_4)_{0.5}(C_4H_8N_2H_3)[V_4(HPO_3)_7(H_2O)_3]\bullet 1.5H_2O$ (**1**) **(a)** Before, and **(b)** After electrochemistry

(b) $(H_3NCH_2CH_2NH_3)_4[V^{III}(H_2O)_2(V^{IV}O)_6(OH)_2(HP\ O_4)_3(PO_4)_5]\bullet 3H_2O$ (2)

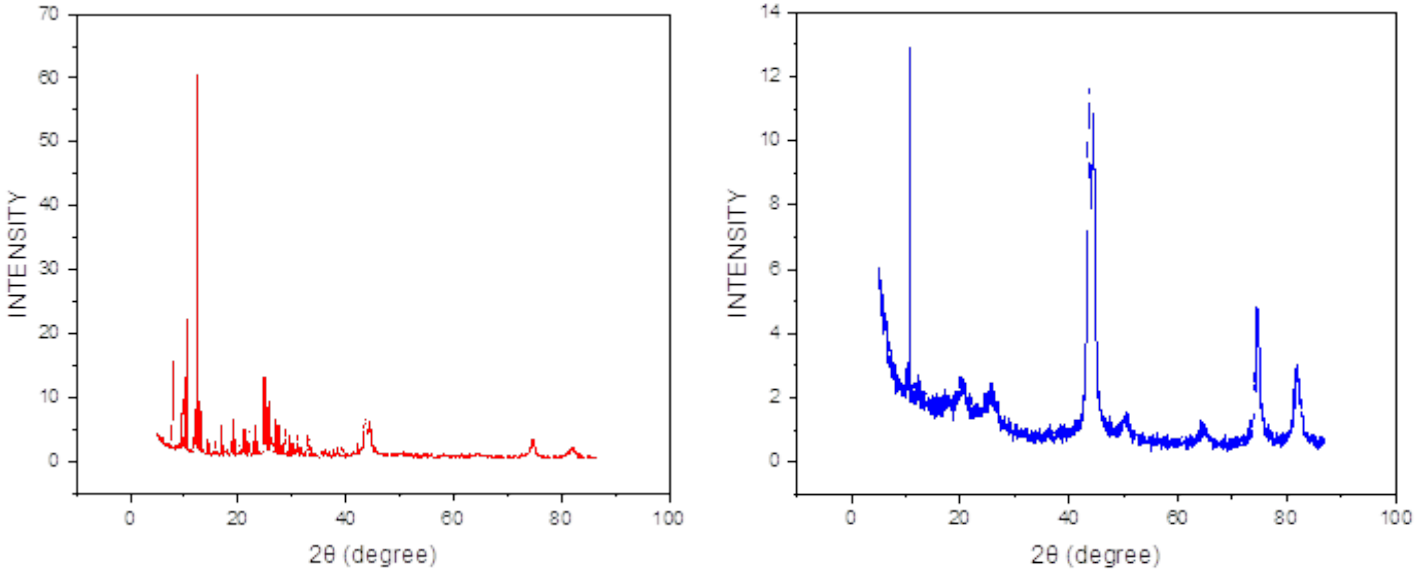

(a) **(b)**

Figure 3.9: PXRD pattern of electrode material $(H_3NCH_2CH_2NH_3)_4[V^{III}(H_2O)_2(V^{IV}O)_6(OH)_2(HP\ O_4)_3(PO_4)_5]\bullet 3H_2O$ **(2) (a)** Before, and **(b)** After electrochemistry

CHAPTER 4: CONCLUSION

4. CONCLUSION

In conclusion, the comparative electrochemical analysis of the homo-valent and mixed-valent oxo-vanado-phosphate compounds reveals key insights into their catalytic behavior and efficiency. The homo-valent compound, $(C_4H_{10}N_2H_2)_{0.5}(C_4H_{10}N_2H)[V^{III}_4(HPO_3)_7(H_2O)_3]\bullet 1.5H_2O$ (**1**) exhibits a lower overpotential for water oxidation, indicating a more energetically favorable pathway for initiating catalytic current. This compound also shows narrower cyclic voltammetry (CV) peak separations, suggesting more reversible redox transitions and efficient electron transfer kinetics. These features point to greater electrochemical stability and a lower energy barrier for catalysis, making it highly suitable for sustained, energy-efficient water oxidation.

In contrast, the mixed-valent compound $(H_3NCH_2CH_2NH_3)_4[V^{III}(H_2O)_2(V^{IV}O)_6(OH)_2(HPO_4)_3(PO_4)_5]\bullet 3H_2O$ (**2**), presents broader and more intense catalytic waves in the CV, indicative of strong catalytic activity and a higher number of electrons transferred during the reaction. It also achieves higher current densities, reflecting improved catalytic turnover once activated. However, this compound suffers from a larger CV peak separation, implying slower electron transfer kinetics and reduced electrochemical reversibility. Moreover, the higher overpotential required to initiate catalysis suggests a greater energy demand, potentially limiting efficiency under operational conditions.

Overall, while the mixed-valent compound is advantageous for generating higher catalytic currents, the homo-valent compound offers superior performance in terms of onset potential (or overpotential), reversibility, and energy efficiency. These findings suggest that the homo-valent compound is better suited for initiating and sustaining efficient catalytic cycles at lower energy costs, whereas the mixed-valent compound may be more effective in applications prioritizing high throughout over energy conservation.